

# MLPG Method for Transient Heat Conduction Problem with MLS as Trial Approximation in Both Time and Space Domains

D. Mirzaei<sup>1</sup> and M. Dehghan<sup>1</sup>

**Abstract:** The meshless local Petrov-Galerkin (MLPG) method with an efficient technique to deal with the time variable are used to solve the heat conduction problem in this paper. The MLPG is a meshless method which is (mostly) based on the moving least squares (MLS) scheme to approximate the trial space. In this paper the MLS is used for approximation in both time and space domains, and we avoid using the time difference discretization or Laplace transform method to overcome the time variable. The technique is applied for continuously nonhomogeneous functionally graded materials (FGM) in a finite strip and a hollow cylinder. This idea can be easily extended to all MLS based methods such as the element free Galerkin (EFG), the local boundary integral equation (LBIE) and etc.

**Keywords:** Meshless methods, Moving least squares (MLS) approximation, MLPG method, Heat conduction problem, Functionally graded materials (FGM).

## 1 Introduction

There are several approaches for numerical solution of boundary value problems. Finite difference (FD) methods, finite elements methods (FEM), spectral methods and boundary elements method (BEM) are some of such technologies. While these methods have been successfully applied to wide ranges of engineering problems, meshless methods are in their own way to be another powerful approach. Meshless methods are based on approximation in terms of scattered data (Belytschko, Krongauz, Organ, Fleming, and Krysl (1996)). Moving least squares (MLS) is one of the scattered data approximation methods, that has been used successfully to approximate the trial space in plenty of meshless methods. For instance we can mention element-free Galerkin (EFG) method (Belytschko, Lu, and Gu (1994)),

---

<sup>1</sup> Department of Applied Mathematics, Faculty of Mathematics and Computer Science, Amirkabir University of Technology, No. 424, Hafez Ave., 15914, Tehran, Iran.

Email addresses: d\_mirzaei@aut.ac.ir (D. Mirzaei), mdehghan@aut.ac.ir (M. Dehghan).

boundary nodes method (BNM) (Mukherjee and Mukherjee (1997)), meshless local boundary integral equation (LBIE) method (Zhu, Zhang, and Atluri (1998)), meshless local Petrov-Galerkin (MLPG) method (Atluri and Zhu (1998)) and etc. Meshless methods are becoming popular, due to their high adaptivity and a low cost to prepare input data for numerical analysis. The latest, MLPG, introduced by Atluri and his colleagues (Atluri and Zhu (1998); Atluri and Shen (2002); Atluri (2005)), has got more interest which is based on local sub-domains, rather than a global domain, and requires neither domain elements nor background cells in either the approximation or the integration. These properties make the MLPG a *truly* weak-based meshless method. Several types of MLPG have been presented and labeled from 1 up to 6. This classification allows some other meshless methods to be especial cases of the MLPG (Atluri and Shen (2002); Atluri (2005)).

Meshless methods have been employed for solving transient heat conduction problems in many papers. For example you can see Sladek, Sladek, and Zhang (2003); Sladek, Sladek, Krivacek, and Zhang (2003); Sladek, Sladek, and Atluri (2004); Sladek, Sladek, and Zhang (2004); Sladek, Sladek, Tanaka, and Zhang (2005); Sladek, Sladek, and Zhang (2005); Qian and Batra (2005); Ling and Atluri (2006); Wang, Qin, and Kang (2006); Sladek, Sladek, Hellmich, and Eberhardsteiner (2007); Sladek, Sladek, Tan, and Atluri (2008) and etc.

Also there are many time-dependent problems considered by meshless methods. For instance you can see Dehghan and Mirzaei (2008a,b); Feng, Han, and Li (2009); Mirzaei and Dehghan (2010b); Abbasbandy and Shirzadi (2010, 2011) and etc.

In all of these papers the meshless methods are used to approximate the space variable. Authors have employed either the time discretization or the Laplace transform techniques to eliminate the time variable in differential equation.

In this paper, we propose an interesting method which employs MLS for approximation in both time and space domains. Although the technique is presented for the MLPG method, it can be easily extended to other meshless methods.

This paper is organized as follows. In the rest of the section we will introduce some general notations and definitions that we will refer to them in next sections. Section 2 is devoted to a brief review of MLS approximation. In Section 3, we will discretize the heat conduction problem using MLS approximations for both time and space variables. In Section 4, some notes on polynomial basis functions are given. In Section 5, numerical results will be presented and finally in Section 6 the article ends with a brief conclusion.

Given the multi-index  $\alpha = (\alpha_1, \dots, \alpha_d) \in \mathbb{N}_0^d$ ,  $|\alpha|$  denotes the sum  $\alpha_1 + \dots + \alpha_d$ ,

and, if  $u$  is sufficiently smooth function,  $D^\alpha u$  denotes the partial derivative

$$\frac{\partial^{|\alpha|}}{\partial \bar{x}_1^{\alpha_1} \dots \partial \bar{x}_d^{\alpha_d}} u.$$

Also  $x^\alpha = \bar{x}_1^{\alpha_1} \bar{x}_2^{\alpha_2} \dots \bar{x}_d^{\alpha_d}$  where  $x = (\bar{x}_1, \bar{x}_2, \dots, \bar{x}_d) \in \mathbb{R}^d$ .

The *unisolvency* condition is required not only for MLS approximation but also for every multivariate approximation method. A set  $X = \{x_1, x_2, \dots, x_N\}$  of pairwise distinct centers is called  $\mathbb{P}_m^d$ -*unisolvant* if the zero polynomial is the only polynomial from  $\mathbb{P}_m^d$  which vanishes at all centers  $x_j$ .

In the MLS and other scattered data approximation methods two quantities *fill distance* (or *mesh-size*) and *separation distance* are important to measure the quality of centers and derive the rate of convergence. For a set of points  $X = \{x_1, x_2, \dots, x_N\}$  in a bounded domain  $\Omega \subseteq \mathbb{R}^d$  the fill distance  $h_X$  is the radius of the largest ball which is completely contained in  $\Omega$  and the separation distance  $q_X$  is the largest possible radius for two balls centered at different data points to be essentially disjoint. They can be defined as

$$h_X = \sup_{x \in \Omega} \min_{1 \leq j \leq N} \|x - x_j\|_2, \quad q_X = \frac{1}{2} \min_{i \neq j} \|x_i - x_j\|_2.$$

A set  $X$  of data sites is said to be *quasi-uniform* with respect to a constant  $c_{qu} > 0$  if  $q_X \leq h_X \leq c_{qu} q_X$ .

## 2 MLS approximation

In this section, we discuss the moving least squares (MLS) that will be used for approximation in both time and space variables in heat conduction problem.

The MLS approximation can be defined as bellow: Let  $u \in C(\Omega)$ , having the data set  $\{u(x_j)\}$  for  $1 \leq j \leq N$  at point set  $X = \{x_1, x_2, \dots, x_N\} \subset \Omega \subset \mathbb{R}^d$ , the MLS approximation of  $u(x)$  can be written as

$$\hat{u}(x) = \sum_{j=1}^N a_j(x) u(x_j).$$

We assume this approximation is exact for a finite dimensional subspace  $S = \text{span}\{p_1, p_2, \dots, p_Q\}$ , i.e.

$$\sum_{j=1}^N a_j(x) p(x_j) = p(x), \quad p \in S.$$

In MLS, we are interested in local approximation. To be more precise we choose a continuous function  $\phi : [0, \infty) \rightarrow [0, \infty)$  with

- $\phi(r) > 0, 0 \leq r < 1,$
- $\phi(r) = 0, r \geq 1,$

and define

$$w_\delta(x, y) = \phi\left(\frac{\|x - y\|_2}{\delta}\right),$$

for  $\delta > 0$  as a weight function. We further define the set of indices

$$J := J(x, \delta, X) = \{j \in \{1, 2, \dots, N\} : \|x - x_j\|_2 \leq \delta\},$$

of centers contained in the interior of closed ball  $B(x, \delta)$  of radius  $\delta$  around  $x$  and use  $S = \mathbb{P}_m^d$  as a space of  $d$ -variate polynomials of degree at most  $m$  of dimension  $Q = \binom{m+d}{d}$ . According to these assumptions the MLS approximation to  $u(x)$  is defined as  $\hat{u}(x) := p^*(x)$ , where  $p^*$  is the solution of

$$\min \left\{ \sum_{j \in J} (u(x_j) - p(x_j))^2 w_\delta(x, x_j) : p = \sum_{k=1}^Q b_k p_k \right\}, \tag{1}$$

According to Levin (1998) and Wendland (2001, 2005),  $p^*$  can be written as

$$p^*(x) = \sum_{j \in J} a_j^*(x) u(x_j),$$

where  $a_j^*(x)$  minimize the quadratic form

$$\frac{1}{2} \sum_{j \in J} a_j^2 \theta_\delta(x, x_j),$$

subject to the linear constraints

$$\sum_{j \in J} a_j p_k(x_j) = p_k(x), \quad 1 \leq k \leq Q,$$

where  $\theta_\delta = 1/w_\delta$ . The functions  $a_j^*$  are called MLS shape functions. From the definition of MLS shape functions, if  $w_\delta \in C^k(\Omega)$  then  $\hat{u}(x) \in C^k(\Omega)$ . Existence and uniqueness of MLS shape functions were considered in Levin (1998), Theorem 2.1 of Wendland (2001) and Theorem 4.3 and Corollary 4.4 of Wendland (2005).

The approximation is well-defined if the unisolvency condition satisfies. If we define the matrix

$$P = (p_\ell(x_j)), \quad 1 \leq \ell \leq Q, \quad j \in J,$$

then the unisolvent condition means that  $P$  is full-rank. A necessary condition is  $|J| \geq Q$ , i.e. there should be at least  $Q$  points in the support of weight function  $w_\delta$  (the domain of definition of MLS approximation), but these conditions are not sufficient. The necessary and sufficient condition is however the unisolvent condition. When  $d = 1$ , every set of distinct points with condition  $|J| \geq Q$  is a  $\mathbb{P}_m^1$ -unisolvent set. The unisolvent condition in multivariate cases ( $d \geq 2$ ) is not as straight forward as univariate one. But for some especial cases we can conclude the unisolvent. Some of these cases can be found in Theorem 2.7 and Lemma 2.8. of Wendland (2005).

In computations, it is better to rewrite the MLS approximation in the matrix-vector form. According to minimization problem (1) and using the standard optimization theory, if we set

$$\begin{aligned} \mathbf{p}(x) &= [p_1(x), p_2(x), \dots, p_Q(x)], \\ \mathbf{a}^*(x) &= [a_1^*(x), a_2^*(x), \dots, a_N^*(x)], \\ W(x) &:= (\delta_{jk} w_\delta(x, x_k))_{j,k \in J(x)}, \end{aligned}$$

then

$$\mathbf{a}^*(x) = \mathbf{p}(x)A^{-1}B, \quad (2)$$

where  $A(x) = PW(x)P^T$  and  $B(x) = PW(x)$ . In an extended form we have

$$a_j^*(x) = \sum_{k=1}^Q p_k(x) [A^{-1}(x)B(x)]_{kj}, \quad 1 \leq j \leq N. \quad (3)$$

It is easy to show that  $A$  is a positive definite matrix, and so invertible. This matrix sometimes is called the *moment matrix* and plays an important role in the MLS approximation. We will come back to this matrix in Section 4.

The error analysis of MLS approximation can be found in Armentano (2001); Levin (1998); Wendland (2001, 2005); Zuppa (2003). Under some conditions, for all  $u \in C^{m+1}(\Omega)$  and quasi-uniform point set  $X$  with fill distance  $h_X$  we have  $\|u - \hat{u}\|_\infty \approx O(h_X^{m+1})$ .

The order of convergence of MLS approximation mainly depends on the polynomial basis  $\{p_1, \dots, p_Q\}$  and the quality of point set  $X$ . It dose not depend on the weight function. The weight function is used to make a *moving* and *local* approximation. But weight may stabilize the approximation. Here, the following  $C^\infty$  Gaussian weight function is used:

$$w_\delta(x, x_j) = \begin{cases} \frac{\exp[-(d_j/c)^2] - \exp[-(\delta/c)^2]}{1 - \exp[-(\delta/c)^2]}, & 0 \leq d_j \leq \delta, \\ 0, & d_j > \delta, \end{cases}$$

where  $d_j = \|x - x_j\|_2$ ,  $c = c_0 h_X$  is a constant controlling the shape of the weight function and  $\delta = \delta_0 h_X$  is the size of the support domain, with constants  $c_0$  and  $\delta_0$ . The derivatives of  $\hat{u}(x)$  can be written as

$$D^\alpha \hat{u}(x) = \sum_{j \in J} D^\alpha a_j^*(x) u(x_j), \tag{4}$$

where

$$D^\alpha a_j^*(x) = \sum_{k=1}^Q D^\alpha \left( p_k(x) [A^{-1}(x)B(x)]_{kj} \right),$$

where  $D^{e_i} A^{-1} = -A^{-1} (D^{e_i} A) A^{-1}$ , and so on. Note that  $e_i = (0, \dots, 0, 1, 0, \dots, 0) \in \mathbb{N}_0^d$  where 1 is in  $i$ -th place. The convergence rates of MLS derivatives of order  $|\alpha| \leq m$  can be also found in Armentano (2001); Zuppa (2003). In this case the order of convergence is  $O(h_X^{m+1-|\alpha|})$ .

If we set

$$\psi_j(x) = \begin{cases} a_j^*(x), & j \in J, \\ 0, & \text{otherwise,} \end{cases} \tag{5}$$

the MLS approximation can be written as

$$\hat{u}(x) = \sum_{j=1}^N \psi_j(x) u(x_j), \tag{6}$$

that will refer to it as MLS approximation equation in the following.

### 3 Heat conduction problem

Let  $\Omega \subset \mathbb{R}^d$  be a bounded  $d$  dimensional domain. The governing equation of the heat conduction problem can be written as

$$\frac{1}{\alpha(x)} \frac{\partial u}{\partial t}(x, t) = \Delta u(x, t) + \frac{1}{\kappa(x)} \nabla \kappa(x) \cdot \nabla u(x, t) + \frac{1}{\kappa(x)} f(x, t), \tag{7}$$

where  $x \in \Omega$  and  $0 \leq t \leq t_F$  denote the time and the space variables, respectively, and  $t_F$  is the final time. The initial and boundary conditions are

$$u(x, 0) = u_0(x), \quad x \in \Omega, \tag{8}$$

$$u(x, t) = \bar{u}(x, t), \quad x \in \Gamma_u, \quad 0 \leq t \leq t_F, \tag{9}$$

$$\kappa(x) \frac{\partial u}{\partial n}(x, t) = \bar{q}(x, t), \quad x \in \Gamma_q, \quad 0 \leq t \leq t_F. \tag{10}$$

In (7)-(10),  $\Delta$  represents the Laplacian operator,  $u(x, t)$  is the temperature field,  $\kappa(x)$  and  $\alpha(x)$  stand for the thermal conductivity and diffusivity, respectively, and  $f(x, t)$  is the density of the body heat sources. Moreover  $n$  is the unit outward normal to the boundary  $\Gamma$ ,  $\bar{u}$  and  $\bar{q}$  are specified values on the Dirichlet boundary  $\Gamma_u$  and Neumann boundary  $\Gamma_q$  where  $\Gamma = \Gamma_u \cup \Gamma_q$ .

To employ the MLS approximation in time domain, we do the following: from (7) and (8) we have

$$\frac{1}{\alpha} u(x, t) = \int_0^t \left[ \Delta u(x, \tau) + \frac{1}{\kappa} \nabla \kappa \cdot \nabla u(x, \tau) \right] d\tau + \frac{1}{\kappa} \int_0^t f(x, \tau) d\tau + \frac{1}{\alpha} u_0(x), \quad (11)$$

keeping in mind  $\alpha := \alpha(x)$  and  $\kappa := \kappa(x)$  are some functions of space variable  $x$ . First the MLS approximation is written in respect to the time variable  $t$ . The idea comes up from the MLS based method for Fredholm and Volterra integral equations presented in Mirzaei and Dehghan (2010a). Here the Volterra type is compatible.

Consider  $F$  distinct points  $T = \{t_1, t_2, \dots, t_F\}$  in the time domain  $[0, t_F]$ , with the fill distance  $h_T$ . It is better  $t_F$  be included because in various cases we need the solution at the final time. According to (6), replacing  $x$  by  $t$  and  $N$  by  $F$ , the univariate MLS approximation to equation (11) in respect to the time variable  $t$ , after imposing at  $t = t_k$  for  $1 \leq k \leq F$ , is

$$\begin{aligned} \frac{1}{\alpha} \sum_{\ell=1}^F \psi_{\ell}(t_k) u(x, t_{\ell}) - \sum_{\ell=1}^F \left( \int_0^{t_k} \psi_{\ell}(\tau) d\tau \right) \left( \Delta u(x, t_{\ell}) + \frac{1}{\kappa} \nabla \kappa \cdot \nabla u(x, t_{\ell}) \right) \\ = \frac{1}{\kappa} \int_0^{t_k} f(x, \tau) d\tau + \frac{1}{\alpha} u_0(x). \end{aligned} \quad (12)$$

The integrations over  $[0, t_k]$  can be done by converting this interval to interval  $[0, 1]$  using the following linear transformation

$$\tau(t, \theta) = t\theta. \quad (13)$$

Therefore if we set

$$\begin{aligned} E_{k,\ell} &= \psi_{\ell}(t_k), \quad 1 \leq k, \ell \leq F, \\ G_{k,\ell} &= \int_0^{t_k} \psi_{\ell}(\tau) d\tau = t_k \int_0^1 \psi_{\ell}(t_k \theta) d\theta = t_k \sum_{j=1}^M \psi_{\ell}(t_k \theta_j) \omega_j, \quad 1 \leq k, \ell \leq F, \\ \mathbf{u}(x) &= [u(x, t_1), \dots, u(x, t_F)], \\ \mathbf{f}(x) &= [f_1(x), \dots, f_F(x)], \quad f_k(x) = t_k \sum_{j=1}^M f(x, t_k \theta_j) \omega_j, \quad 1 \leq k \leq F, \\ \mathbf{u}_0(x) &= [u_0(x), \dots, u_0(x)]_{1 \times F}, \end{aligned} \quad (14)$$

where  $\{\theta_j, \omega_j\}_{j=1}^M$  is a  $M$ -point Gauss quadrature (or others) formula in  $[0, 1]$ , then we have

$$\frac{1}{\alpha} E \mathbf{u}^T(x) - G \left( \Delta \mathbf{u}^T(x) + \frac{1}{\kappa} [\nabla \kappa \cdot \nabla \mathbf{u}(x)]^T \right) = \frac{1}{\kappa} \mathbf{f}^T(x) + \frac{1}{\alpha} \mathbf{u}_0^T(x). \tag{15}$$

In addition from Dirichlet boundary condition (9), we have

$$\sum_{\ell=1}^F \psi_\ell(t_k) u(x, t_\ell) = \bar{u}(x, t_k), \quad 1 \leq k \leq F, \quad x \in \Gamma_u,$$

and if we set  $\bar{\mathbf{u}}(x) = [\bar{u}(x, t_1), \dots, \bar{u}(x, t_F)]$ , then

$$E \mathbf{u}^T(x) = \bar{\mathbf{u}}^T(x), \quad x \in \Gamma_u. \tag{16}$$

Moreover, from the Neumann boundary condition (10), we have

$$\sum_{\ell=0}^F \psi_\ell(t_k) \frac{\partial u}{\partial n}(x, t_\ell) = \frac{1}{\kappa} \bar{q}(x, t_k), \quad 1 \leq k \leq F, \quad x \in \Gamma_q$$

and if we set  $\bar{\mathbf{q}}(x) = [\bar{q}(x, t_1), \dots, \bar{q}(x, t_F)]$ , then

$$E \frac{\partial \mathbf{u}^T}{\partial n}(x) = \frac{1}{\kappa} \bar{\mathbf{q}}^T(x), \quad x \in \Gamma_q. \tag{17}$$

Consider Equations (15)-(17), now we have a time free system of equations. Our goal is applying the MLPG method (here the MLPG5) to solve this problem. Thus the MLS approximation in respect to the space variable  $x$  should be applied. According to the MLPG process, first the local weak forms are written over local sub-domains  $\Omega_\sigma^y \subset \Omega$  where  $\partial \Omega_\sigma^y = L_\sigma^y \cup \Gamma_\sigma^y$ , and  $\Gamma_\sigma^y$  is a part of sub-domain's boundary which has intersection with global boundary  $\Gamma$  over which the Neumann boundary conditions are applied. The local sub-domains could be of any geometric shape and size. For simplicity they are taken to be  $B(y, \sigma) \cap \bar{\Omega}$ . Note that neither Lagrange multiplier nor penalty parameters are introduced in the local weak form, because the Dirichlet boundary conditions are imposed directly using the MLS approximation. It is clear that for every internal node  $y$ ,  $\Gamma_\sigma^y = \emptyset$  and  $L_\sigma^y = \partial \Omega_\sigma^y$ . From (15) and (17) we have

$$\begin{aligned} E \int_{\Omega_\sigma^y} \frac{1}{\alpha} \mathbf{u}^T(x) d\Omega - G \int_{L_\sigma^y} \frac{\partial \mathbf{u}^T}{\partial n}(x) d\Gamma - G \int_{\Omega_\sigma^y} \left( \frac{1}{\kappa} [\nabla \kappa \cdot \nabla \mathbf{u}(x)]^T \right) d\Omega \\ = \int_{\Omega_\sigma^y} \left[ \frac{1}{\kappa} \mathbf{f}^T(x) + \frac{1}{\alpha} \mathbf{u}_0(x) \right] d\Omega + G E^{-1} \int_{\Gamma_\sigma^y} \frac{1}{\kappa} \bar{\mathbf{q}}^T(x) d\Gamma \end{aligned} \tag{18}$$

that is held for every  $y \in \text{int}(\Omega) \cup \Gamma_q$ , providing  $E$  is an invertible matrix. As we know,  $E$  is the MLS shape function matrix and due to the theory of MLS approximation it is nonsingular. The right hand side of Equation (18) is a known vector of size  $F \times 1$ , say  $\mathbf{r}(y)$ . For  $y \in \Gamma_u$ , Equation (16) is repeated replacing  $x$  by  $y$ .

Now consider the set of  $\mathbb{P}_m^d$ -unisolvant and quasi-uniform  $X = \{x_1, x_2, \dots, x_N\}$  in  $\Omega$  with fill distance  $h_X$ . For simplicity suppose that  $x_j \in \Gamma_u$  for  $1 \leq j \leq N_1$  and  $x_j \in \Gamma_q \cup \text{int}(\Omega)$  for  $N_1 + 1 \leq j \leq N$ . Thanks to the MLS approximation, the vectors  $\mathbf{u}$  and its derivatives can be written in terms of values of  $\mathbf{u}$  at the point set  $X$ . To make difference between the MLS approximation in time and space, here we use the notation  $\phi_j(x)$  instead of  $\psi_j(x)$  for shape functions in (6). Thus equation (16) can be approximated by

$$E \left( \sum_{j=1}^N \phi_j(y) \mathbf{u}^T(x_j) \right) = \bar{\mathbf{u}}^T(y), \quad y \in \Gamma_u. \quad (19)$$

and equation (18) by

$$\begin{aligned} E \left( \sum_{j=1}^N \left[ \int_{\Omega_\sigma^y} \frac{1}{\alpha} \phi_j(x) d\Omega \right] \mathbf{u}^T(x_j) \right) - G \left( \sum_{j=1}^N \left[ \int_{L_\sigma^y} \frac{\partial \phi_j}{\partial n}(x) d\Gamma \right] \mathbf{u}^T(x_j) \right) \\ - G \left( \sum_{j=1}^N \left[ \int_{\Omega_\sigma^y} \frac{1}{\kappa} \nabla \kappa \cdot \nabla \phi_j(x) d\Omega \right] \mathbf{u}^T(x_j) \right) = \mathbf{r}(y). \end{aligned} \quad (20)$$

Holding (19) at  $y = x_i$ ,  $1 \leq i \leq N_1$  and (20) at  $y = x_i$ ,  $N_1 + 1 \leq i \leq N$  and setting

$$\begin{aligned} H_1(i, j) &= \phi_j(x_i), \quad 1 \leq i \leq N_1, \quad 1 \leq j \leq N, \\ H_2(i, j) &= \int_{\Omega_\sigma^{x_i}} \frac{1}{\alpha(x)} \phi_j(x) d\Omega, \quad N_1 + 1 \leq i \leq N, \quad 1 \leq j \leq N, \\ K_2(i, j) &= \int_{L_\sigma^{x_i}} \frac{\partial \phi_j}{\partial n}(x) d\Gamma + \int_{\Omega_\sigma^{x_i}} \frac{1}{\kappa} \nabla \kappa \cdot \nabla \phi_j(x) d\Omega, \quad N_1 + 1 \leq i \leq N, \quad 1 \leq j \leq N, \\ R_1(i, :) &= \bar{\mathbf{u}}(x_i), \quad N_1 + 1 \leq i \leq N, \\ R_2(i, :) &= \mathbf{r}(x_i), \quad N_1 + 1 \leq i \leq N, \\ U(j, :) &= \mathbf{u}(x_j), \quad 1 \leq j \leq N, \end{aligned} \quad (21)$$

give

$$\begin{cases} E(H_1 U)^T &= R_1^T \\ E(H_2 U)^T - G(K_2 U)^T &= R_2^T \end{cases}$$

Let  $H = [H_1^T H_2^T]_{N \times N}$ ,  $K = [0 K_2^T]_{N \times N}$  and  $R = [R_1^T R_2^T]_{F \times N}$ , thus we have

$$EU^T H - GU^T K = R, \tag{22}$$

which is a *generalized Sylvester* equation. This equation should be solved by some linear algebra techniques that we will discuss in the following. Note that  $U(j, \ell) = u(x_j, t_\ell)$  for  $1 \leq j \leq N$  and  $1 \leq \ell \leq F$ . When  $U$  is derived from equation (22), the solution at every point  $(x, t) \in \Omega \times [0, t_F]$  can be approximated by

$$u(x, t) \approx \hat{u}(x, t) = \sum_{j=1}^N \phi_j(x) u(x_j, t) = \sum_{j=1}^N \sum_{\ell=1}^F \phi_j(x) \psi_\ell(t) u(x_j, t_\ell).$$

If we set

$$\Phi(x) = [\phi_1(x), \dots, \phi_N(x)], \quad \Psi(t) = [\psi_1(t), \dots, \psi_F(t)],$$

then

$$u(x, t) \approx \Phi(x)U\Psi^T(t). \tag{23}$$

Note that,  $E$  and  $G$  are time and  $H$  and  $K$  are space matrices. The method provides the time and space matrices separately. Therefore other meshless methods in space can be easily replaced by the MLPG, presented in this paper.

However, this method needs a linear algebra technique for numerically solving the generalized Sylvester equation (22). There are several strategies.

This equation can be converted to

$$TU^T + U^T S = C, \tag{24}$$

with the time matrix  $T = G^{-1}E$ , the space matrix  $S = -KH^{-1}$  and the right-hand side  $C = G^{-1}RH^{-1}$ , providing  $G$  and  $H$  are invertible matrices. Equation (24) is a *standard Sylvester* equation with unknown  $U$ . In MATLAB the function

$$X = \text{lyap}(T, S, -C)$$

gives the solution  $U = X^T$ . Numerical results show, the matrix  $H$  is invertible and if 0 is not included in  $T$ , the matrix  $G$  is also invertible. Note that there is no force to include zero.

Another technique is based on invertibility of at least one of matrices  $E$ ,  $H$ ,  $G$  or  $K$ . As we know  $E$ , the MLS shape function matrix, is nonsingular. The pair of equations

$$\begin{cases} L_1 H + G L_2 = R \\ L_1 K + E L_2 = 0 \end{cases} \tag{25}$$

are equivalent to (22) with  $EU^T = L_1$  and  $U^TK = -L_2$ . This system is a *coupled standard Sylvester equation*. Recovering  $L_1$  from (25),  $U^T = E^{-1}L_1$ .

Equation (22) can also be solved directly, without any assumption on invertibility of matrices, using the Bartels-Stewart (BS) or Hessenberg-Schur (HS) algorithms presented in Gardiner, Laub, Amato, and Moler (1992) based on QZ factorization. In these algorithms a transformation method is used which employs the QZ algorithm to structure the equation in such a way that it can be solved column-wise by a back substitution technique. Gardiner, Laub, Amato, and Moler (1992) derived: if  $N \geq F$  (if is not change  $N$  and  $F$ ), the computational costs of BS and HS algorithms are

$$\text{BS} : 33N^3 + 33F^3 + 3N^2F + 3F^2N,$$

$$\text{HS} : 8.8N^3 + 33F^3 + (5 + 5.5p)N^2F + 3F^2N,$$

where  $0 \leq p \leq 0.5$ . This means that the computational costs of both methods are  $O(N^3 + F^3)$ . As we will see, solving a generalized Sylvester equation in this method is not a noticeable problem in sense of computational costs in comparison to other time elimination techniques.

Note that some iteration algorithms can be also used for solving generalized Sylvester equations. For more details see Dehghan and Hajarain (2011) and the references therein.

The results of this paper are performed using the Bartels-Stewart (BS) or Hessenberg-Schur (HS) algorithms.

In time discretization method we can use a difference equation of order  $O(\Delta t)$  like  $[u(x, t + \Delta t) - u(x, t)]/\Delta t$  instead of  $\partial u/\partial t$ . If we suppose  $u(x, n\Delta t) = u^{(n)}(x)$  and approximate  $u$  by  $\theta u^{(n+1)} + (1 - \theta)u^{(n)}$  for  $0 < \theta \leq 1$ , Equations (7)-(10) after imposing the MLS approximation convert to

$$\begin{bmatrix} H_1 \\ \theta K_2 - \frac{1}{\Delta t} H_2 \end{bmatrix} \mathbf{u}^{(n+1)} = \begin{bmatrix} \mathbf{b}_1^{(n+1)} \\ -((1 - \theta)K_2 + \frac{1}{\Delta t} H_2) \mathbf{u}^{(n)} + \mathbf{b}_2^{(n+1)} \end{bmatrix}, \quad (26)$$

where  $H_1$ ,  $H_2$  and  $K_2$  are defined in (21) and

$$\mathbf{b}_1^{(n)}(i) = \bar{u}^{(n)}(x_i), \quad 1 \leq i \leq N_1,$$

$$\mathbf{b}_2^{(n)}(i) = - \int_{\Gamma_{\sigma}^{x_i}} \frac{1}{\kappa(x)} \bar{q}(x, n\Delta t) d\Gamma - \int_{\Omega_{\sigma}^{x_i}} \frac{1}{\kappa(x)} f(x, n\Delta t) d\Omega, \quad N_1 + 1 \leq i \leq N.$$

System (26) should be solved for  $n = 0, 1, 2, \dots, M$  with  $u^{(0)}(x_i) = u_0(x_i)$  till getting the desirable time  $t = M\Delta t$ . If  $\Delta t$  chosen to be constant in all time steps, the stiffness matrix is constant and LU decomposition, once, (costing  $O(N^3)$  operators) and

backward and forward substitutions,  $M$  times, (costing  $O(MN^2)$  operators) require. In this case a small time step  $\Delta t$  needs to get accurate results. In the method of this paper the order of convergence in the time domain is  $O(h_T^{m+1})$ , therefore  $F$  (the number of time MLS points) can be chosen absolutely smaller than  $M$ .

Laplace transform method is another way to solve the time dependent problems. Suppose that  $\mathcal{L}u(t) = \tilde{u}(s)$ . Applying  $\mathcal{L}$  on both sides of Equations (7)-(10) and doing the MLS approximation for  $\tilde{u}(x, s)$  in respect to variable  $x$ , yield

$$\begin{bmatrix} H_1 \\ K_2 - sH_2 \end{bmatrix} \tilde{\mathbf{u}}(s) = \begin{bmatrix} \mathbf{b}_1(s) \\ \mathbf{b}_0 + \mathbf{b}_2(s) \end{bmatrix}, \tag{27}$$

where  $H_1, H_2$  and  $K_2$  are defined in (21) and

$$\mathbf{b}_1(i) = \tilde{u}(x_i), \quad 1 \leq i \leq N_1,$$

$$\mathbf{b}_0(i) = - \int_{\Omega_\sigma^{x_i}} \frac{1}{\alpha(x)} u_0(x) d\Omega, \quad N_1 + 1 \leq i \leq N,$$

$$\mathbf{b}_2(i) = - \int_{\Gamma_\sigma^{x_i}} \frac{1}{\kappa(x)} \tilde{q}(x, s) d\Gamma - \int_{\Omega_\sigma^{x_i}} \frac{1}{\kappa(x)} \tilde{f}(x, s) d\Omega, \quad N_1 + 1 \leq i \leq N.$$

Finally a numerical Laplace inversion technique requires, that needs solutions of (27) for many  $s$ . The stiffness matrix depends on  $s$  and should be solved as well as  $s$  changes. This means that several linear system of equations should be solved to get the solution at a sample time  $t$ . Moreover, Laplace transforms of the body force and the boundary conditions should be provided. Also, the accuracy of the space method (here MLPG) will finally lose due to the poor accuracies of Laplace inversion techniques.

#### 4 Some notes on basis functions in MLS

Before going to numerical problems, we give some explanations to polynomial basis  $\{p_1, \dots, p_Q\}$ . Practically authors use the set

$$\{x^\alpha\}_{0 \leq |\alpha| \leq m}, \tag{28}$$

as a basis function for  $\mathbb{P}_m^d$  in the MLS approximation. The choice of this basis is important and has influence especially on matrix  $A = PWP^T$ . Matrix  $A$  should be a well-posed matrix because the accuracy of computing  $A^{-1}$  in (3) must be guaranteed. This matrix is positive definite and thus nonsingular. But numerical results show that when the density of nodes increases (or more precisely  $h_X$  and  $q_X$  decrease) the determinant of  $A$  decreases rapidly and the accuracy of computing  $A^{-1}$  gets worse due to the roundoff errors. This phenomenon effects the final numerical

results and we will have a numerical instability in the algorithms of MLS based methods.

To overcome this drawback it is better to use the *shifted scaled basis polynomials* (Mirzaei, Schaback, and Dehghan (2011)). The shifted basis can be defined by

$$\{(x-z)^\alpha\}_{0 \leq |\alpha| \leq m}, \quad (29)$$

and the shifted scaled basis by

$$\left\{ \frac{(x-z)^\alpha}{q_X^{|\alpha|}} \right\}_{0 \leq |\alpha| \leq m}, \quad (30)$$

where  $q_X$  is the separation distance and  $z$  is a fixed evaluation point such as a test point or a Gaussian point for integration in weak-form based techniques. We use the notations  $A = P^T W P$  where the basis (28) is employed and  $A^z = P(\cdot - z)^T W P(\cdot - z)$  and  $A_{q_X}^z = P(\frac{\cdot - z}{q_X})^T W P(\frac{\cdot - z}{q_X})$  where (29) and (30) are used respectively. It can be proved that  $\det(A) = \det(A^z)$ . In addition, we set

$$D = \text{diag} \left\{ 1, \underbrace{\frac{1}{q_X}, \dots, \frac{1}{q_X}}_{\binom{d}{d-1} \text{ times}}, \underbrace{\frac{1}{q_X^2}, \dots, \frac{1}{q_X^2}}_{\binom{d+1}{d-1} \text{ times}}, \dots, \underbrace{\frac{1}{q_X^m}, \dots, \frac{1}{q_X^m}}_{\binom{d-1+m}{d-1} \text{ times}} \right\}_{Q \times Q}.$$

It is clear that  $A_{q_X}^z = D A^z D$ , hence

$$\det(A_{q_X}^z) = \det(A^z) [\det(D)]^2 = \det(A) [\det(D)]^2.$$

Using the combinatorial formula

$$\sum_{j=0}^m j \binom{d-1+j}{d-1} = d \binom{d+m}{d+1} =: \rho,$$

we have  $\det(D) = q_X^{-\rho}$ , therefore

$$\det(A_{q_X}^z) = q_X^{-2\rho} \det(A),$$

and this is the reason why the determinant of  $A_{q_X}^z$  remains constant as  $q_X$  decreases. Using the shifted scaled basis, matrix  $A$  becomes well-conditioned and  $A^{-1}$  is computed accurately. The quantity  $q_X$  can be replaced by a function which varies in accordance with node density in  $\Omega$ .

**5 Numerical results**

In this section, first, we examine and compare the proposed technique using a simple test problem. Then the method is applied for analyzing transient heat conduction in nonhomogeneous functionally graded materials (FGMs), which has a continuously functionally graded thermal conductivity parameter. Due to the high mathematical complexity of the initial boundary value problems, analytical approaches for the thermomechanics of FGMs are restricted to simple geometry and boundary conditions. Thus, the transient heat conduction analysis in FGM demands accurate and efficient numerical methods (Sladek, Sladek, Tan, and Atluri (2008)). In numerical results, we use the quadratic shifted scaled basis polynomial functions ( $m = 2$ ) in the MLS approximation for both time and space domains. For integration over the local sub-domains in MLPG (space) a ten points Gauss formula is used. For the time integration (for generation the matrix  $G$ ), if the time domain is large it is better to use more accurate quadratures. Here we use a fifty points Gauss formula. If the time domain is small we can use some fewer points quadrature formulas.

**5.1 Test Problem**

Let  $\Omega = [0, 1]^2 \subset \mathbb{R}^2$  and consider Equations (7)-(10) with  $\alpha = 1/(2\pi^2)$ ,  $\kappa = 1$  and  $f(x, t) = 0$ . The function  $u(x, t) = \exp(-t) \cos(\pi x_1) \cos(\pi x_2)$  satisfies to such equation. Initial and essential boundary conditions are extracted accordingly. Here, we compare the results of MLPG5, with time difference scheme and MLS approximation in time, in terms of maximum errors and CPU times used. To be fair in comparison, let  $F = M$ ,  $\Delta t = h_T$  and  $t_F = 5$ . As we can see from the results presented in Table 1, MLPG with MLS in time is more accurate than MLPG with time difference scheme. The Sylvester equation is solved using Bartels-Stewart (BS) algorithm, and the final linear system of time difference method is decomposed using LU technique once and then backward and forward substitutions give the solutions at other time levels. Table 1 shows that the CPU times used are approximately the same for both techniques. This confirms the discussions presented at the end of Section 3.

Table 1  
Comparison of “Time difference” and “MLS in time” schemes with  $\Delta t = h_T = 0.5$ .

$N$	Time difference		MLS in time	
	$\ e\ _\infty$	CPU time used	$\ e\ _\infty$	CPU time used
36	$6.5 \times 10^{-3}$	3.7 Sec.	$2.9 \times 10^{-3}$	3.7 Sec.
121	$3.6 \times 10^{-3}$	25.0	$8.8 \times 10^{-4}$	24.3
441	$3.2 \times 10^{-3}$	125.5	$5.7 \times 10^{-4}$	127.0

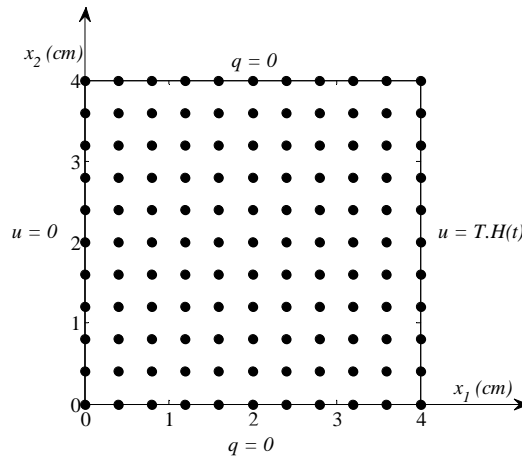


Figure 1: Boundary conditions and node distribution for a finite strip.

In the next problems we will see the superiority of this method over Laplace transform technique in terms of accuracy.

### 5.2 Problem 1 in FGM

In two dimensional case ( $d = 2$ ), consider a finite strip with a unidirectional variation of the thermal conductivity and diffusivity. The same exponential spatial variation for both parameters is taken

$$\begin{aligned}\kappa(x) &= \kappa_0 \exp(\gamma x_1), \\ \alpha(x) &= \alpha_0 \exp(\gamma x_1),\end{aligned}\tag{31}$$

with  $\alpha_0 = 0.17 \times 10^{-4} \text{ m}^2\text{s}^{-1}$  and  $\kappa_0 = 17 \text{ Wm}^{-1}\text{deg}^{-1}$ . Three different exponential parameters  $\gamma = 0.2, 0.5$  and  $1.0 \text{ cm}^{-1}$  ( $20, 50$  and  $100 \text{ m}^{-1}$ ) are selected in numerical calculation. On both opposite sides parallel to the  $x_2$ -axis two different temperatures are prescribed. One side is kept to zero temperature and the other has the Heaviside step time variation i.e.,  $u = T_0 H(t)$  with  $T_0 = 1 \text{ deg}$ . On the lateral sides of the strip the heat flux vanishes. See Fig. 1.

Such problem has considered in Sladek, Sladek, and Zhang (2003) using meshless LBIE method with Laplace transform in time and in Wang, Qin, and Kang (2006) using a meshless collocation method with time difference approximation.

In numerical calculations, a square with a side-length  $a = 0.04 \text{ m}$  and a  $11 \times 11$  regular node distribution is used for the MLS approximation in the space domain (Fig.

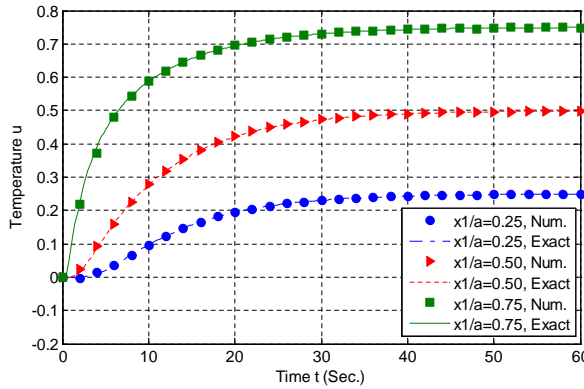


Figure 2: Time variation of the temperature in a finite strip at three positions with  $\gamma = 0$

1). Also a regular node distribution in the time domain  $t \in [0, 60]$  with  $h_T = 3$  is used. After solving the final Sylvester system for  $U$  at the collocation points in time and space, the values of unknown function  $u$  at other points  $(x, t)$  are approximated using equation (23).

The special case with an exponential parameter  $\gamma = 0$  corresponds to a homogeneous material. In such a case an analytical solution is available

$$u(x, t) = \frac{T_0 x_1}{a} + \frac{2}{\pi} \sum_{n=1}^{\infty} \frac{T_0 \cos n\pi}{n} \sin \frac{n\pi x_1}{a} \times \exp\left(-\frac{\alpha_0 n^2 \pi^2 t}{a^2}\right),$$

which can be used to check the accuracy of the present numerical method. Numerical results are computed at three locations along the  $x_1$ -axis with  $x_1/a = 0.25, 0.5$  and  $0.75$ . Results are depicted in Fig. 2. An excellent agreement between numerical and analytical results is obtained.

The discussion above concerns heat conduction in homogeneous materials only since analytical solutions can be used for verification. To illustrate the application of the proposed algorithm, consider now the cases  $\gamma = 0.2$ , and  $0.5 \text{ cm}^{-1}$ , respectively. The variation of temperature with time for three  $\gamma$ -values and at position  $x_1 = 0.01$  and  $0.02$  m are presented in Figs. 3 and 4, respectively.

Fig. 4 is in good agreement with the Figure 11 presented in Wang, Qin, and Kang (2006), but some differences are evident between Fig. 3 and Figure 4 of Sladek, Sladek, and Zhang (2003). This disagreement also was reported in Table 1 of Wang, Qin, and Kang (2006). Note that in this case our results are in agreement with Table 1 of Wang, Qin, and Kang (2006).

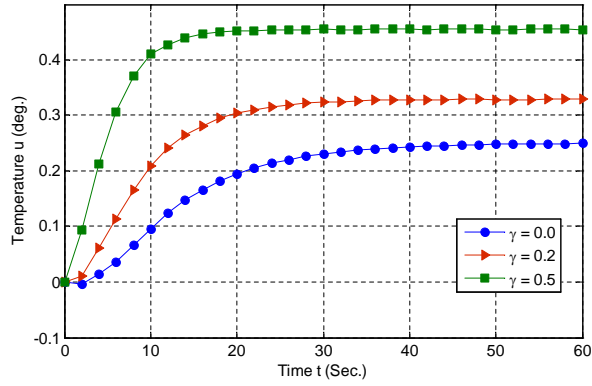


Figure 3: Time variation of the temperature at position  $x_1/a = 0.25$  of the functionally graded finite strip

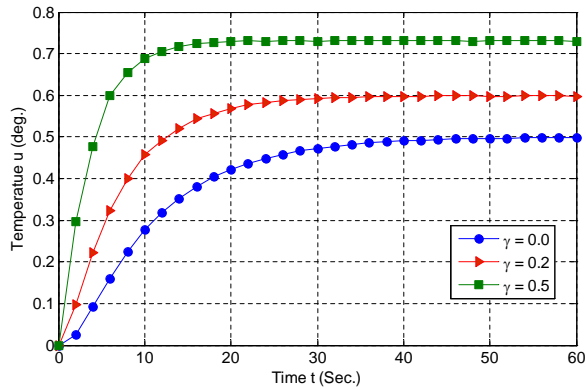


Figure 4: Time variation of the temperature at position  $x_1/a = 0.5$  of the functionally graded finite strip

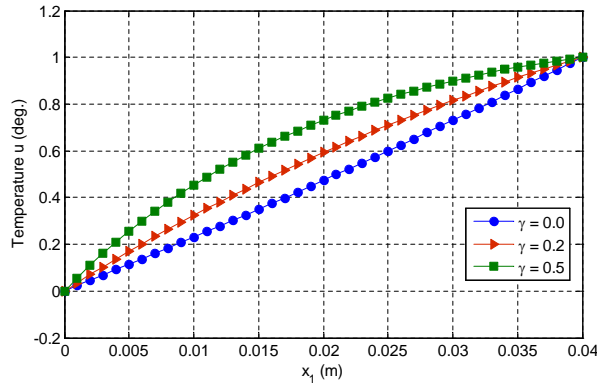


Figure 5: Distribution of temperature at  $t = 30$  s along  $x_1$ -axis of functionally graded finite square strip

Fig. 5 shows the distribution of temperature along the  $x_1$ -axis at  $t = 30$  sec. This figure again is in very good agreement with the corresponding Figure 12 of Wang, Qin, and Kang (2006). As expected, it is found from Figs. 3, 4 and 5 that the temperature increases along with an increase in  $\gamma$ -values (or equivalently in thermal conductivity), and the temperature approaches a steady state when  $t > 20$  sec.

For final steady state an analytical solution can be obtained as

$$u(x, t \rightarrow \infty) = T_0 \frac{\exp(-\gamma x_1) - 1}{\exp(-\gamma a) - 1}, \left( u \rightarrow T \frac{x_1}{a}, \text{ as } \gamma \rightarrow 0 \right).$$

Analytical and numerical results computed at time  $t = 60$  sec. corresponding to stationary or static loading conditions are presented in Fig. 6. The numerical results are in good agreement with the analytical results for the steady state case.

### 5.3 Problem 2 in FGM

In this example, an infinitely long and functionally graded thick-walled hollow cylinder is considered, where the following radii  $R_1 = 8 \times 10^{-2}$  m and  $R_2 = 10 \times 10^{-2}$  m are selected. This problem is considered in Sladek, Sladek, and Zhang (2003) using meshless LBIE method. The Laplace transform is employed to overcome the time variable.

Heaviside step boundary condition is prescribed on the external surface of the hollow cylinder for the time-dependent thermal loading as a thermal shock with  $T_0 = 1$  deg. The inner surface is kept at zero temperature. Due to the symmetry in geometry and boundary conditions it is sufficient to analyze only a quarter of the cross

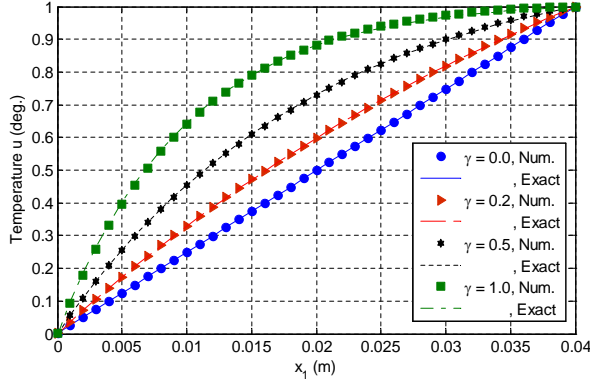


Figure 6: Distribution of temperature along  $x_1$ -axis for a functionally graded finite square strip under steady-state loading conditions

section of the hollow cylinder. The boundary conditions and the total nodes lying in the domain and on the global boundary are depicted in Fig. 7.

The thermal conductivity and diffusivity functions are chosen such as (31) with same constants  $\alpha_0$  and  $\kappa_0$ . For comparison purpose, a homogeneous material ( $\gamma = 0$ ) is first considered. In this homogeneous case, an analytical solution is known as:

$$u(r, t) = T_0 \frac{\ln(r/R_1)}{\ln(R_2/R_1)} - \pi \sum_{n=1}^{\infty} T_0 \frac{J_0^2(R_1 \beta_n) U_0(r \beta_n)}{J_0^2(R_1 \beta_n) - J_0^2(R_2 \beta_n)} \times \exp(-\alpha_0 \beta_n^2 t),$$

where

$$U_0(r \beta_n) = J_0(r \beta_n) Y_0(R_2 \beta_n) - J_0(R_2 \beta_n) Y_0(r \beta_n),$$

and  $\beta_n$  are the roots of the following transcendental equation

$$J_0(r) Y_0(r R_2 / R_1) - Y_0(r) J_0(r R_2 / R_1) = 0,$$

with  $J_0(r)$  and  $Y_0(r)$  being Bessel functions of first and second kinds and zeroth order. In numerical results we use time step  $h_T = 1$  in the time domain  $[0, 16]$  and after solving the final Sylvester system for  $U$  at collocation points in time and space, the values of unknown function  $u$  are approximated using equation (23). Fig. 8 depicts the numerical and exact solutions in various times at  $r = 9$  cm. The results show an excellent agreement with the analytical solution.

Fig. 9 shows the variation of the temperature with radial coordinate at four different time instants.

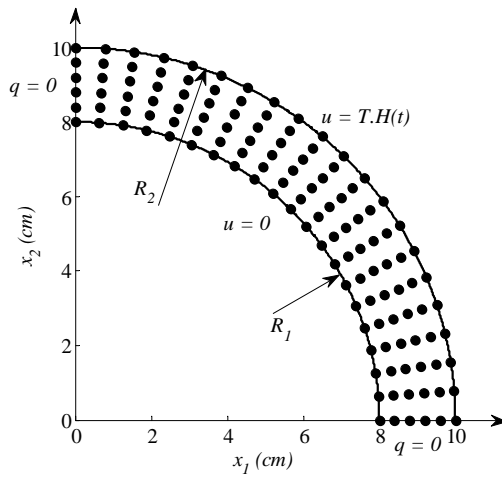


Figure 7: Boundary conditions and node distribution for a hollow cylinder.

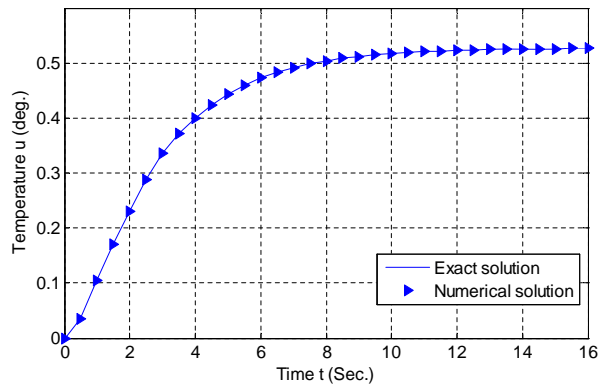


Figure 8: Exact and numerical solution at  $r = 9$  cm in hollow cylinder with homogeneous material properties ( $\gamma = 0$ ).

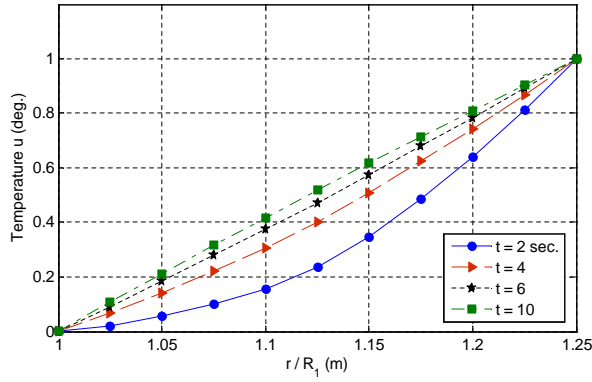


Figure 9: Temperature variation with radial coordinate  $r$  in hollow cylinder at different time levels with homogeneous material properties ( $\gamma = 0$ ).

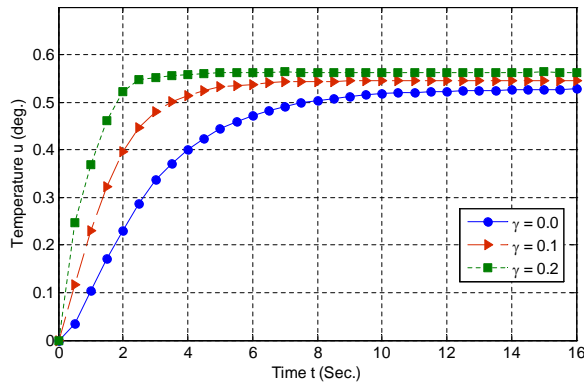


Figure 10: Time variation of the temperature at  $r = 9$  cm in a functionally graded hollow cylinder

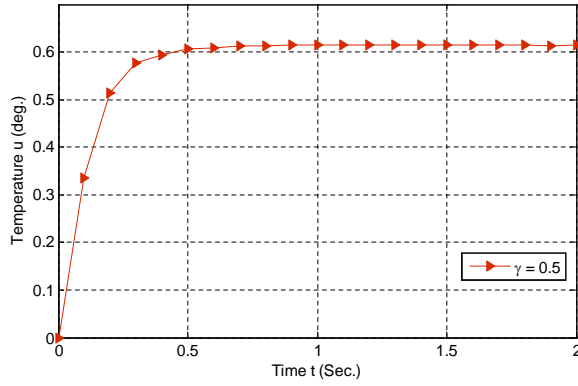


Figure 11: Time variation of the temperature at  $r = 9$  cm for  $\gamma = 0.5 \text{ cm}^{-1}$  for a functionally graded hollow cylinder.

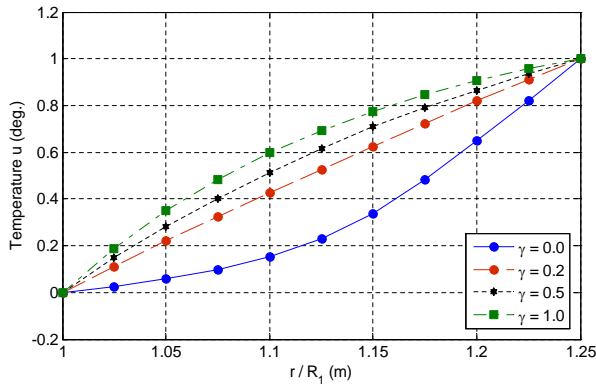


Figure 12: Temperature variation with radial coordinate  $r$  at  $t = 2$  sec. for a functionally graded hollow cylinder

Finally, we consider the functionally graded hollow cylinder with the thermal diffusivity and conductivity being graded in the radial direction. Numerical results for the time variation of the temperature are shown in Fig. 10. Similar to the results for a finite strip in the first example, the temperature level at interior points in the steady state increases with increasing  $\gamma$ -value. Here, again there is a difference between the results of this paper and the results presented in Figure 9 of Sladek, Sladek, and Zhang (2003) using meshless LBIE method and Laplace transform. It can be seen that the results of this paper are larger than those obtained by LBIE method for inhomogeneous case. This difference also observed in the previous example. For  $\gamma = 0.5$  the temperature grows rapidly and gets the steady-state in lower times. To analyze this case we use the very fine time step  $h_T = 0.1$ . The results are presented in Fig. 11. As we see, for  $t > 1$  sec., we get the steady state solution.

Finally Fig. 12 illustrates the variation of the temperature with the normalized radial coordinate  $r/R_1$  for different choices of  $\gamma$  at  $t = 2$  sec.

## 6 Conclusion

This article describes a numerical implementation of meshless methods, such as MLPG, to transient heat conduction problem. We use the MLS method for approximation in both time and space domains. The scheme leads to a generalized Sylvester equation. This system can be solved using some linear algebra techniques with  $O(N^3 + F^3)$  operations, where  $N$  and  $F$  are the numbers of meshless points in the space domain  $\Omega$  and the time domain  $[0, t_F]$ , respectively. Finally some applications are provided to the transient heat conduction analysis in continuously nonhomogeneous functionally graded materials (FGM). Although the process has presented for the MLPG method, we can extend this idea to other MLS based meshless methods, similarly.

**Acknowledgement:** The authors deeply thank Dr. Behnam Hashemi (Shiraz University of Technology, Iran) for his valuable remarks and suggestions on the generalized Sylvester equation.

## References

- Abbasbandy, S.; Shirzadi, A.** (2010): A meshless method for two-dimensional diffusion equation with an integral condition. *Engineering Analysis with Boundary Elements*, vol. 34, pp. 1031–1037.
- Abbasbandy, S.; Shirzadi, A.** (2011): MLPG method for two-dimensional diffusion equation with neumann's and non-classical boundary conditions. *Applied Numerical Mathematics*, vol. 61, pp. 179–180.

**Armentano, M.** (2001): Error estimates in Sobolev spaces for moving least square approximations. *SIAM Journal on Numerical Analysis*, vol. 39(1), pp. 38–51.

**Atluri, S.; Zhu, T.-L.** (1998): A new meshless local Petrov-Galerkin (MLPG) approach in Computational mechanics. *Computational Mechanics*, vol. 22, pp. 117–127.

**Atluri, S. N.** (2005): *The meshless method (MLPG) for domain and BIE discretizations*. Tech Science Press, Encino, CA.

**Atluri, S. N.; Shen, S.** (2002): *The Meshless Local Petrov-Galerkin (MLPG) Method*. Tech Science Press, Encino, CA.

**Belytschko, T.; Krongauz, Y.; Organ, D.; Fleming, M.; Krysl, P.** (1996): Meshless methods: an overview and recent developments. *Computer Methods in Applied Mechanics and Engineering, special issue*, vol. 139, pp. 3–47.

**Belytschko, T.; Lu, Y.; Gu, L.** (1994): Element-Free Galerkin methods. *International Journal for Numerical Methods in Engineering*, vol. 37, pp. 229–256.

**Dehghan, M.; Hajarian, M.** (2011): Analysis of an iterative algorithm to solve the generalized coupled Sylvester matrix equations. *Applied Mathematical Modelling*, vol. 35, pp. 3285–3300.

**Dehghan, M.; Mirzaei, D.** (2008): The meshless local Petrov-Galerkin (MLPG) method for the generalized two-dimensional non-linear Schrödinger equation. *Engineering Analysis with Boundary Elements*, vol. 32, pp. 747–756.

**Dehghan, M.; Mirzaei, D.** (2008): Numerical solution to the unsteady two-dimensional Schrödinger equation using meshless local boundary integral equation method. *International Journal for Numerical Methods in Engineering*, vol. 76, pp. 501–520.

**Feng, W.; Han, X.; Li, Y.** (2009): Fracture analysis for two-dimensional plane problems of nonhomogeneous magneto-electro-thermo-elastic plates subjected to thermal shock by using the meshless local Petrov-Galerkin method. *CMES: Computer Modeling in Engineering and Sciences*, vol. 48, no. 1, pp. 1–26.

**Gardiner, G.; Laub, A.; Amato, J.; Moler, C.** (1992): Solution of the Sylvester matrix equation  $AXB^T + CXD^T = E$ . *AMS Transactions on Mathematical Software*, vol. 18, no. 2, pp. 223–231.

**Levin, D.** (1998): The approximation power of moving least-squares. *Mathematics of Computation*, vol. 67, pp. 1517–1531.

**Ling, X.; Atluri, S.** (2006): Stability analysis for inverse heat conduction problems. *CMES: Computer Modeling in Engineering and Sciences*, vol. 13, no. 3, pp. 219–228.

- Mirzaei, D.; Dehghan, M.** (2010): A meshless based method for solution of integral equations. *Applied Numerical Mathematics*, vol. 60, pp. 245–262.
- Mirzaei, D.; Dehghan, M.** (2010): Meshless local Petrov-Galerkin (MLPG) approximation to the two dimensional sine-Gordon equation. *Journal of Computational and Applied Mathematics*, vol. 233, pp. 2737–2754.
- Mirzaei, D.; Schaback, R.; Dehghan, M.** (2011): On generalized moving least squares and diffuse derivatives. *Submitted*.
- Mukherjee, Y.; Mukherjee, S.** (1997): The boundary node method for potential problems. *International Journal for Numerical Methods in Engineering*, vol. 40, pp. 797–815.
- Qian, L.; Batra, R.** (2005): Three-Dimensional transient heat conduction in a functionally graded thick plate with a higher-order plate theory and a meshless local Petrov-Galerkin method. *Computational Mechanics*, vol. 35, pp. 214–226.
- Sladek, J.; Sladek, V.; Atluri, S.** (2004): Meshless local Petrov-Galerkin method for heat conduction problem in an anisotropic medium. *CMES: Computer Modeling in Engineering and Sciences*, vol. 6, pp. 309–318.
- Sladek, J.; Sladek, V.; Hellmich, C.; Eberhardsteiner, J.** (2007): Heat conduction analysis of 3-D axisymmetric and anisotropic FGM bodies by meshless local Petrov-Galerkin method. *Computational Mechanics*, vol. 39, pp. 223–233.
- Sladek, J.; Sladek, V.; Krivacek, J.; Zhang, C.** (2003): Local BIEM for transient heat conduction analysis in 3-D axisymmetric functionally graded solids. *Computational Mechanics*, vol. 32, pp. 169–176.
- Sladek, J.; Sladek, V.; Tan, C.; Atluri, S.** (2008): Analysis of transient heat conduction in 3D anisotropic functionally graded solids, by the MLPG method. *CMES: Computer Modeling in Engineering and Sciences*, vol. 32, no. 3, pp. 161–174.
- Sladek, J.; Sladek, V.; Tanaka, M.; Zhang, C.** (2005): Transient heat conduction in anisotropic and functionally graded media by local integral equations. *Engineering Analysis with Boundary Elements*, vol. 29, pp. 1047–1065.
- Sladek, J.; Sladek, V.; Zhang, C.** (2003): Transient heat conduction analysis in functionally graded materials by the meshless local boundary integral equation method. *Computational Materials Science*, vol. 28, pp. 494–504.
- Sladek, J.; Sladek, V.; Zhang, C.** (2004): A local BIEM for analysis of transient heat conduction with nonlinear source terms in FGMs. *Engineering Analysis with Boundary Elements*, vol. 28, pp. 1–11.

**Sladek, J.; Sladek, V.; Zhang, C.** (2005): Stress analysis in anisotropic functionally graded materials by the MLPG method. *Engineering Analysis with Boundary Elements*, vol. 29, pp. 597–609.

**Wang, H.; Qin, Q.-H.; Kang, Y.-L.** (2006): A meshless model for transient heat conduction in functionally graded materials. *Computational Mechanics*, vol. 38, pp. 51–60.

**Wendland, H.** (2001): Local polynomial reproduction and moving least squares approximation. *IMA Journal of Numerical Analysis*, vol. 21, pp. 285–300.

**Wendland, H.** (2005): *Scattered Data Approximation*. Cambridge University Press.

**Zhu, T.; Zhang, J.; Atluri, S.** (1998): A local boundary integral equation (LBIE) method in computational mechanics, and a meshless discretization approach. *Computational Mechanics*, vol. 21, pp. 223–235.

**Zuppa, C.** (2003): Error estimates for moving least square approximations. *Bulletin of the Brazilian Mathematical Society*, vol. 34(2), pp. 231–249.